Not to appear in Nonlearned J., 45.
Preprint typeset using LaTeX style emulateapj v. 6/22/04

A KEPLERIAN GASEOUS DISK AROUND THE B0 STAR R MON

A. Fuente[1], T. Alonso-Albi[1], R. Bachiller[1], A. Natta[2], L. Testi[2], R. Neri[3], P. Planesas[1]

Not to appear in Nonlearned J., 45.

ABSTRACT

We present high-angular resolution observations of the circumstellar disk around the massive Herbig Be star R Mon (M_*∼8 $M_\odot$) in the continuum at 2.7mm and 1.3mm and the ^{12}CO 1→0 and 2→1 rotational lines. Based on the new 1.3mm continuum image we estimate a disk mass (gas+dust) of 0.007 $M_\odot$ and an outer radius of <150 AU. Our CO images are consistent with the existence of *a Keplerian rotating gaseous disk around this star*. Up to our knowledge, this is the most clear evidence for the existence of Keplerian disks around massive stars reported thus far. The mass and physical characteristics of this disk are similar to those of the more evolved T Tauri stars and indicate a shorter timescale for the evolution and dispersal of circumstellar disks around massive stars which lose most of their mass before the star becomes visible.

Subject headings: Radio continuum: stars – Circumstellar matter – Stars: individual (R Mon) – Stars: pre-main sequence

1. INTRODUCTION

Herbig Ae/Be stars (HAEBE) are intermediate mass (M∼2–10 $M_\odot$) pre-main sequence objects. A big theoretical and observational effort has been done in recent years for the understanding of the disk occurrence and evolution in HAEBE. For Herbig Ae and late-type Be stars (spectral type later than B7) (hereafter HAE), it is generally accepted the presence of disks similar to those associated with T Tauri stars (TTs). The association of the more massive early Be stars (HBE) with disks is more uncertain. Evidence for the existence of dusty and gaseous circumstellar disks around some HBE exists at optical, NIR and mid-IR wavelengths (Meeus et al. 2001,Vink et al. 2002, Millan-Gabet et al. 2001, Acke et al. 2005). Furthermore, disks around HBE seem to have different geometry from those around HAE and TTs. While most HAE and TTs have flared disks, HBE seem to have (if any) geometrically flat disks (see e.g. Acke et al. 2005). However, the direct detection of circumstellar disks around HBE at millimeter wavelengths has remained elusive until recently.

We carried out a high sensitivity search for circumstellar disks around HBE with the aim of studying the frequency and time-scales of disks in these massive stars. We observed a sample of HBE in the continuum at mm- and cm- wavelengths using the PdBI and VLA (Fuente et al. 2001; Fuente et al. 2003, hereafter Paper I) and detected two dusty disks around MWC 1080 and R Mon with total (gas+dust) masses of ∼0.003 $M_\odot$ and ∼0.01 $M_\odot$ respectively. These were the first detections of dusty disks in HBE.

R Mon is a very young HBE with a T Tauri companion separated by 0.69″. Because of its youth, R Mon is not directly visible in the optical but appears as a resolved conical reflection nebula in scattered light. At infrared wavelengths, R Mon appears as a point source located 0.06"±0.02 south from the optical peak. Close et al. (1997) measured an extinction of A_v=13.1 mag towards the star that they interpreted as due to an optically thick disk of radius, r_{out}=100 AU. Our previous VLA and PdBI images of R Mon at 1.3cm, 0.7cm and 2.7mm showed a compact source located ∼0.45" south from the optical position (Paper I). Based on these interferometric observations we derived a mass of 0.01 $M_\odot$ for the dusty disk. R Mon hosts the most massive disk detected in HBE so far and it is the best candidate to study disks around massive stars. In this paper, we present observations at higher angular resolution and sensitivity of the R Mon disk in the continuum at 3mm and 1.3mm and in the ^{12}CO rotational lines. Our ^{12}CO observations are consistent with the existence of a gaseous disk in Keplerian rotation around the star.

2. OBSERVATIONS

We present high-angular resolution observations in the continuum at 115.3 GHz and 230.5 GHz and in the ^{12}CO 1→0 and 2→1 lines towards the B0 star R Mon. The ^{12}CO observations were carried out with the IRAM[4] array at Plateau de Bure (PdBI) from 2003, December to 2004, March in the C and A configuration providing a beam of 2.28"×1.27" at 115.3 GHz and 1.47"×0.94" at 230.5 GHz. The absolute flux density scale was determined from measurements on MWC349, 0420-014 and 0528+134. The maps were not corrected for primary beam attenuation. During 2006, January we carried out continuum observations of this source using the new A^+ configuration of PdBI. These observations provide a beam of 1.28"×0.83" at 2.7mm and 0.72"×0.33" at 1.3mm. All the images are centered at R.A.= 06:39:09.95, Dec=+08:44:09.6 (J2000).

3. CONTINUUM IMAGES

The new high angular resolution continuum images are presented in Fig. 1ab. These images provide a more accurate position for the disk that now is settled

[1] Observatorio Astronómico Nacional (OAN), Apdo. 112, E-28803 Alcalá de Henares (Madrid), Spain
[2] INAF-Osservatorio Astrofisico de Arcetri, Largo Enrico Fermi 5, I-50125 Firenze, Italy
[3] Institute de Radioastronomie Millimétrique, 300 rue de la Piscine, 38406 St Martin d'Heres Cedex, France
Electronic address: a.fuente@oan.es

[4] IRAM is supported by INSU/CNRS (France), MPG (Germany) and IGN (Spain).

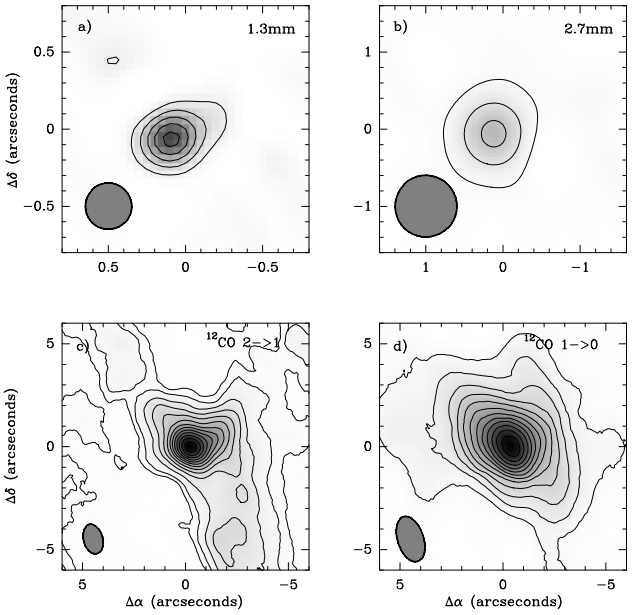

FIG. 1.— Fig 1ab show the interferometric images of the circumstellar disk around R Mon in the continuum at 1.3mm (a) and 2.7mm (b). Contour levels are 1.5mJy/beam to 8mJy/beam by 1.5mJy/beam in the 1.3mm image and 0.75mJy/beam to 8mJy/beam by 1.5mJy/beam in the 3mm image. The images have been obtained by convolving the clean components with a 0.3" circular beam in the case of the 1.3mm map and a 0.8" circular beam in the case of the 2.7mm image. In Fig. 1cd we show integrated intensity maps of the ^{12}CO 2→1 (c) and ^{12}CO 1→0 (d) rotational lines. The contour levels are 0.25 , 0.5 to 6 by steps of 0.5 Jy/beam km/s in the ^{12}CO 2→1 image and 0.25 to 6 by 0.25 Jy/beam km/s in the ^{12}CO 1→0 image. The beam is drawn in the bottom left corner of each panel.

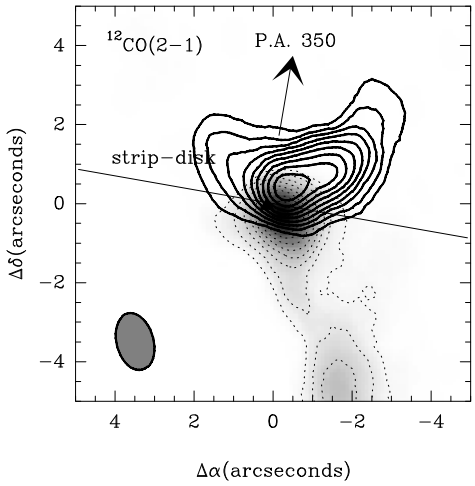

FIG. 2.— Thick contours show the integrated intensity emission of the ^{12}CO 2→1 rotational line in the velocity interval 3.6–7 km/s and dashed contours and grey scale map, the integrated intensity emission in the velocity interval 12-15.4 km/s. The arrow indicates the direction of the outflow axis. The studied strip is drawn in the Figure.

to R.A.=06:39:09.954 Dec=+08:44:09.55 (J2000). The peak emission in the new 2.7mm continuum image is 4.1±0.5 mJy/beam in agreement with our previous measurement published in Paper I. We have detected, for the first time, the R Mon disk at 1.3mm. The peak flux in the 1.3mm image is 7.2±1.0 mJy/beam and the integrated flux is 11.8 mJy. This difference between the peak flux and the integrated flux at 1.3mm suggests a spatial extension of ∼0.3". At the distance of R Mon, this implies a disk radius of ∼150 AU. Our new 1.3mm measurement is consistent with our previous upper limit already discussed in Paper I and implies a spectral index for the dust of β<0.5. The new value of the 1.3mm flux can be used to further constrain the disk mass. After subtracting the free-free emission, we have fitted the emission at millimeter wavelengths assuming thermal dust emission with T_d=215 K (Natta et al. 2000), $\kappa = 0.01(\lambda(mm)/1.3)^{-\beta} cm^{-2} g^{-1}$ and a gas-to-dust ratio of 100 (see more details in Paper I). Our best fit is obtained for a disk with a mass of 0.007 $M_\odot$ and β=0.3–0.5. Values of β between 0.5 and 1 are usually found in circumstellar disks around HAE and TTs and are thought to be evidence for grain growth in these disks (see e.g. Natta et al. 2006). The low value of β in R Mon suggests that grain growth has proceeded to very large sizes already in the short lifetime of its disk.

4. CO IMAGES

We have carried out high angular resolution mapping of the ^{12}CO J=1→0 and J=2→1 lines towards R Mon using the PdBI. Since the interferometer does not sample low spatial frequencies, almost all the flux is missed at the cloud velocities (between 7.0 and 12.0 km s^{-1}). However, intense molecular emission is detected at the velocity intervals of 3.6 km s^{-1}<v<7.0 km s^{-1} and 12.0 km s^{-1}<v<15.6 km s^{-1} (see Fig. 3). These ^{12}CO observations allow us to study in detail the gas kinematics around R Mon.

4.1. *Extended component: The red filament*

In Fig 1cd we present the integrated intensity maps of the ^{12}CO rotational lines. The maps show a compact molecular clump and a more extended weak component. The size of the compact clump in the map of the ^{12}CO 2→1 line is ∼2.5" (2000 AU at a distance of 800 pc). The weak component is extended in the North-South (N-S) direction. Towards the North, its emission presents a parabolic shape following the border of the infrared reflection nebula. Towards the South, the emission is concentrated in an elongated feature. Since the emission at the velocity of the molecular cloud has been filtered out by the interferometer, our integrated intensity maps are actually the sum of the emission of the blue-shifted and red-shifted gas.

In Fig. 2 we show the integrated intensity maps of the emission at blue-shifted and red-shifted velocities separately. The emission presents a clear bipolar morphology with the blue lobe towards the North and the red one towards the South. This N-S distribution is consistent

TABLE 1
MODEL RESULTS*

	Flat disk	Flared disk
Stellar Mass ($M_\odot$)	8±1	8±1
i(°)	20±5	20±5
r_0 (AU)	1	0.8
T_0 (K) (r=r_0)	4500±500	3200±500
q	0.62±0.03	0.66±0.02
M_d ($M_\odot$)	0.014±0.001	0.08±0.01
p	1.3±0.1	0.8±0.1
H(r)		0.33+0.83 r (AU)
Δv_{turb} (km/s)	0.8±0.2	0.0±0.3
$\chi^{2\$}$	1.5	1.8

*Errors are those obtained from the fitting procedure and do not account for other uncertainties inherent in this kind of calculations (instrumental errors, optical depth effects...).

$^\$\chi^2 = \frac{1}{N}\sum_{N,v}\frac{(T_b(model)-T_b(obs))^2}{\sigma^2}$ where N is the number of positions and σ, the rms of each spectrum.

with the morphology of the bipolar outflow at large scale (Cantó et al. 1981, Bachiller et al. 1987). The red lobe presents a jet-like morphology and remains unresolved in the direction perpendicular to it. Jets in radio continuum at 1.3 cm (Paper I) and [SII] emission (Movsessian et al. 2002) have previously been detected in R Mon. However, the direction of the red filament does not coincide with the direction of any of these jets but with the direction of one of the walls of the cavity suggesting that this high velocity emission arises in the entrained gas of the molecular cloud that is being accelerated by the outflow.

4.2. *Compact component: A Keplerian gaseous disk*

A strong compact clump is detected towards the star in the CO images. Our interferometric CO observations allow for the first time to study the kinematics of the molecular gas at the scale of the circumstellar disk. In Fig. 3 we show the Position-Velocity (P-V) diagrams of the emission of the ^{12}CO 1→0 and 2→1 rotational lines in a strip perpendicular to the outflow (see Fig. 2). The P-V diagrams show the characteristic "butterfly" shape of a rotating disk.

We have modeled the emission of the ^{12}CO 1→0 and 2→1 lines to have a deeper insight into the kinematics and physical characteristics of the disk. Our model assumes Local Thermodynamic Equilibrium (LTE), a standard ^{12}CO abundance X(CO)=8 10^{-5} and radial power laws for the gas kinetic temperature and the surface density distribution ($T_k = T_0\ (r/r_0)^{-q}$ and $\Sigma = \Sigma_0\ (r/r_0)^{-p}$).

Since the CO emission has been filtered at the cloud velocities, we have only fitted the high velocity emission (3.6 km s^{-1}<v<7.0 km s^{-1} and 12.0 km s^{-1}<v<15.6 km s^{-1}). Based on NIR and mid-IR observations, several authors have proposed that contrary to HAE and TTs that host flared disks, HBE seem to have geometrically flat disks (see e.g. Acke et al. 2005). We have considered the two different geometries, a flared and a flat disk. The best fit with each geometry is shown in Table 1.

The intensity ratio between the ^{12}CO 1→0 and 2→1 lines is ∼1 as expected for optically thick emission. Since the ^{12}CO lines are optically thick, the "butterfly" shape is only dependent on the gas kinematics regardless of the disk geometry. The observational data are well fitted with a disk in Keplerian rotation around the star. The outer radius of the disk is 1500 AU, the inclination angle 20°±5 and the mass of the star is constrained to 8±1 $M_\odot$. The derived spectral types for R Mon range from B0 (see e.g. Hillenbrand 1992) to B8 (Mora et al. 2001). The stellar mass we obtain is consistent with a star of a spectral type between B0 and B3 but it is larger than that expected for a B8 star. The high gas kinetic temperature derived using both the flat and the flared geometry also supports the classification of R Mon as an early Be star (see Table 1) rather than as a cooler B8 object.

Since the ^{12}CO lines are optically thick, the mass of the gaseous disk is not well determined by our observations. In fact, the estimated value of the mass is strongly dependent on the assumed geometry. Using a flat disk, the best fit is obtained with M_d=0.014 $M_\odot$. A different disk mass is obtained with the flared geometry. In our flared model the height (H) increases linearly with the radius (H ∝ r) and the density is assumed to be constant in the z-direction. These assumptions are reasonable since in hydrostatic equilibrium H ∝ $r^{9/8}$. Moreover, Piétu et al. (2003) based on interferometric CO observations obtained that H ∝ $r^{1.2}$ in the disk around the Ae star HD 34282. We obtain a reasonable fit to the data with H varying from 1 AU (at r=0.8 AU) to 1250 AU (at r=1500 AU), and M=0.08 $M_\odot$. This mass is 10 times larger than that obtained from dust emission and a factor of 6 larger than that obtained from the CO lines assuming a flat disk. This is quite surprising since in TTs and HAE the mass derived from the CO lines (assuming a standard CO abundance) is smaller than that derived from continuum observations (see e.g. Piétu et al. 2003) and suggests that the disk associated with R Mon is very likely flat or at least flatter than those associated with TTs and HAE. This conclusion is also supported by the low value of χ^2 obtained in the case of the flat disk. However, we cannot discard the possibility of a flared disk since the dust emissivity in the disk around R Mon could be smaller than in those around TTs and HAE because of the rapid grain growth and the fit we obtain using the flared disk is still reasonably good.

The values of T_0, q , p and Δv_{turb} are similar in the flat and the flared disk models. Moreover, the values of p, q and Δv_{turb} are similar to those measured in the disks associated with TTs and HAE (see e.g. Dutrey et al. 2004) suggesting that all these stars host disks with similar physical characteristics.

In Fig. 3 and 4 we compare the results of our flat disk model with the observations. The model fits very well the observations in the "red" part of the P-V diagram. However there is a displacement between the observed emission and that predicted by the model in the "blue" part (see Fig. 3 right). The only way to fit the blue part would be to assume an asymmetrical disk and/or an off-center star.

5. DISCUSSION AND CONCLUSIONS

R Mon is the first disk around a HBE detected in molecular lines and so far, our unique opportunity to investigate the physical structure and kinematics of the gas reservoir in the disks associated with these stars. Our most interesting result is that the disk is in Keplerian ro-

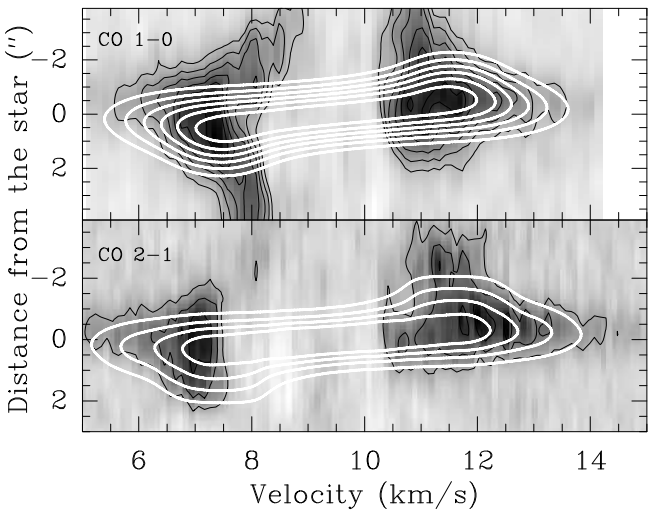

FIG. 3.— Grey scale images are the Position-Velocity (P-V) diagrams of the CO rotational lines along the strip drawn in Fig. 2. White contours show the synthesized P-V diagram with our flat disk model. Contour levels are 200 mJy/beam to 800 mJy/beam in steps of 100 mJy/beam (3.16 K) for the CO 1→0 diagram and 200 mJy/beam to 800 mJy/beam in steps of 200 mJy/beam (3.46 K) for the CO 2→1 one.

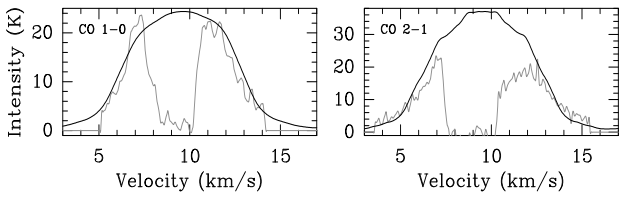

FIG. 4.— Comparison between the spectra observed towards the star position (grey line) and those predicted by our flat disk model (black line). Note that the interferometer misses the flux at the cloud velocities.

tation around the star. Keplerian rotation has also been found in most of the TTs and HAE studied so far and indicates a similar formation mechanisms for the stars in the range 1–8 $M_\odot$. The values obtained for the indexes q and p as well as that for the turbulent broadening are also similar to those found in TTs and some HAE (see e.g. Dutrey et al. 2004). R Mon is a very young object (age$\sim 10^5$ yr) which is still deeply embedded in the molecular cloud. On the contrary, TTs are evolved objects (age$>10^6$ yr) which are not any more associated with the parent molecular core (age$>10^6$ yr). The similarity between the disks of such different objects suggests a shorter timescale for the evolution of the disks associated with HBE. The low occurrence of disks associated with HBE also supports this conclusion. In Paper I we showed that the disk masses in HBe stars are at least an order of magnitude lower than in HAe stars. In fact, the ratio M_d/M_* is roughly constant and equal to 0.04 for stars with spectral type A0-M7 and $M_d/M_* < 0.001$ in HBe stars. This indicates a rapid dispersal of the disk material in HBE.

We have compared the R Mon disk with those associated with massive protostars in order to have a deeper insight into the evolution of disks around HBE. Evidences for circumstellar disks have been found in massive protostars. The surface density in these disks is well described with $p > 2$ (Cesaroni et al. 2005). This means that most of the gas is concentrated at small radii. Recently, Schreyer et al. (2006) detected a 1 $M_\odot$ disk around MWC 490, a 8–10 $M_\odot$ star which is in a transition stage to HBE. In this case, the surface density varies with p=1.5 and the disk radius is 1400 AU. The values of p and r_{out} are similar to those derived in the disk around R Mon. However the mass of the MWC 490 disk is more than an order of magnitude larger than that of the R Mon disk. These results indicate that the disks around HBE flatten and lose a large fraction of their mass ($\sim$90%) before the pre-main sequence phase ($<10^5$ yr). The flattening of the disks can be due to the rapid grain growth. The low value of β measured in R Mon is a clear evidence of the presence of large grains. The grain growth causes the optical depth of the disk to drop and allows the UV radiation to penetrate deep into the circumstellar disk and photo-evaporate the disk external layers (Dullemond & Dominik 2004). Thus, we can propose an evolutionary sequence in which the disks associated with HBE start with a flaring shape but become flat during the pre-main sequence and lose most of their mass (>90%) before the star becomes visible ($<10^5$ yr). The results of this Letter are consistent with this scenario which, however, needs to be confirmed.

This work has been partially supported by the Spanish MEC and Feder funds under grant ESP2003-04957 and by SEPCT/MEC under grants AYA2003-07584 and AYA2002-01055.

REFERENCES

Acke, B., van den Ancker, M. E., & Dullemond, C. P. 2005, A&A, 436, 209
Bachiller, R., Cernicharo, J., & Martín-Pintado, J. 1987, European Regional Astronomy Meeting of the IAU, Volume 4, 29
Cantó, J., Rodríguez, L. F., Barral, J. F., & Carral, P. 1981, ApJ, 244, 102
Cesaroni, R., Neri, R., Olmi, L., Testi, L., Walmsley, C.M., & Hofner, P. 2005, A&A, 434, 1039
Dullemond, C. P., & Dominik, C., 2004, A&A 417, 159
Dutrey, A., Lecavelier Des Etangs, A., & Augereau, J.-C. 2004, Comets II, 81
Close, L.M., Roddier, F., Hora, J.L., Graves, J.E., Northcott, M., Roddier, C., Hoffman, W.F., Dayal, A., Fazio, G.G., Deutsch, L.K., 1997, ApJ, 489, 210
Fuente, A., Neri, R., Martín-Pintado, J., Bachiller, R., Rodríguez-Franco, A., & Palla, F. 2001, A&A, 366, 873
Fuente, A., Rodríguez-Franco, A., Testi, L., Natta, A., Bachiller, R., Neri, R., 2003, ApJL 598, L39 (Paper I)
Hillenbrand, L. A., Strom, S. E., Vrba, F. J., & Keene, J. 1992, ApJ, 397, 613
Meeus, G., Waters, L. B. F. M., Bouwman, J., van den Ancker, M. E., Waelkens, C., & Malfait, K. 2001, A&A, 365, 476
Millan-Gabet, R., Schloerb, F. P., & Traub, W. A. 2001, ApJ, 546, 358
Mora, A., et al. 2001, A&A, 378, 116
Movsessian, T.A., Magakian, T. Yu & Afanasiev V.L., 2002, A&A 390, L5

Natta, A., Grinin, V. P., Mannings, V. 2000, in Protostars and Planets IV, ed. V. Mannings, A. Boss, & S. S. Russell (Tucson: University of Arizona Press), 559
Natta, A., Testi, L., Calvet, N., Henning, T., Waters, R., Wilner, D. 2006, in Protostars and Planets V, in press (astro-ph/0602041).
Piétu, V., Dutrey, A., & Kahane, C. 2003, A&A, 398, 565
Schreyer, K., Semenov, D., Henning, T., & Forbrich, J. 2006, ApJ, 637, L129
Vink, J. S., Drew, J. E., Harries, T. J., & Oudmaijer, R. D. 2002, MNRAS, 337, 356
Weigelt, G., Balega, Y.Y., Hofman, K.-H, Preibisch, T., 2002, A&A 392, 937